Journal of Alloys and Compounds 536S (2012) S265–S270

Contents lists available at SciVerse ScienceDirect

Journal of Alloys and Compounds

journal homepage: www.elsevier.com/locate/jallcom

Exchange bias and magnetic behaviour of iron nanoclusters prepared by the gas aggregation technique

J. Sánchez-Marcos[a], M.A. Laguna-Marco[a], R. Martínez-Morillas[a], F. Jiménez-Villacorta[a,b], E. Céspedes[a], N. Menéndez[c], C. Prieto[a]

[a] Instituto de Ciencia de Materiales de Madrid, Consejo Superior de Investigaciones Científicas, Cantoblanco, 28049 Madrid, Spain
[b] SpLine Spanish CRG Beamline at the European Synchrotron Radiation Facilities, ESRF-BP 220-38043 Grenoble Cedex, France
[c] Dep. Química-Física Aplicada, Universidad Autónoma de Madrid, Cantoblanco, 28049 Madrid, Spain

ARTICLE INFO

Article history:
Received 10 July 2011
Received in revised form 1 December 2011
Accepted 7 December 2011
Available online 16 December 2011

Keywords:
Iron nanoparticles
Exchange bias
Multilayers
Sputtering
Gas aggregation technique

ABSTRACT

Iron nanoclusters have been deposited by the gas-phase aggregation technique to form multilayered structures with outstanding exchange-bias (H_E) values up to H_E = 3300 Oe at low temperatures. In order to explain the observed magnetic properties, composition and crystallographic phase have been determined by X-ray absorption spectroscopy. A metal-oxide core–shell arrangement has to be discarded to explain the large obtained values of H_E since structural results show nanoclusters formed by the antiferromagnetic α-Fe_2O_3 oxide. Moreover, nanoparticles of few nanometers formed by substoichiometric α-Fe_2O_3 explain the observed weak ferromagnetism and let to understand the origin of large exchange bias by the interaction between different spin sublattice configurations provided by the low iron coordination at surface.

1. Introduction

The study of nanometric particles allows new interesting properties. In particular, when the size of ferromagnetic particles tends toward some nanometres, they become single domain and exhibit a number of unique physical properties such giant magnetoresistance, large coercivity, superparamagnetism or quantum tunnelling of magnetization that may provide deep changes in practical applications [1]. Some emerging applications [2] are based on the exchange bias effect [3,4] because of the reduction of saturation fields to observe giant magnetoresistance [5], coercitivity enhancement for permanent magnets [6] or overcome the superparamagnetic limit [7]. From the experimental point of view, after field cooling, those systems present asymmetric hysteresis loops, which are mainly characterized by a shifted loop that is centred at a different from zero magnetic field (H_E) as well as by an increase of coercivity respect to zero field cooling.

Small particles are systems where the surface to volume ratio enhancement activates macroscopic observation of the exchange bias effect. Typically, ferromagnetic (FM) metals covered with their ferri- or antiferromagnetic (AF) native oxide are clear examples of such characteristic. Nevertheless, nanoparticles of ferri- or AF-materials have also been found to show exchange bias [8], which is usually explained by spin disorder at the surface of nanoparticles [9].

From the preparation point of view, several physical vapour deposition techniques allow to obtain nanometric particles. The main characteristic of these nanoparticle production methods is the capability of preparing narrow size distributions of disaggregated nanoparticles with very small size. One of the main advantages of these techniques is the possibility to obtain a small density of nanoparticles on top of substrates allowing magnetic systems formed by non-interacting particles. Often, these methods take advantage of the low thermal energy that inhibits further grain growth at the film growing process on cold substrates after deposition of thermally obtained [10] or sputtered [11] vapours. More recently, the gas-phase aggregation technique has been proven to produce, for instance, cobalt isolated nanoparticles with thermally stable ferromagnetism that overcomes the so-called superparamagnetic limit by the large effective anisotropy between the Co FM core and the CoO AF shell [12].

Typically, cobalt- and iron-based systems prepared by these techniques have been reported to present large anisotropic effects. In this sense, the Co–CoO system has been reported to have one of the largest anisotropic effect ($H_E \sim 10.7$ kOe) for 8 nm size nanoparticles prepared by the vapour deposition technique on water cooled substrates [13] and more recently, 6 nm mean size nanoparticles prepared by the gas-phase aggregation technique present values

E-mail address: sanchej@icmm.csic.es (J. Sánchez-Marcos).

0925-8388/$ – see front matter © 2011 Elsevier B.V. All rights reserved.
doi:10.1016/j.jallcom.2011.12.006

of $H_E \sim 8$ kOe [14]. On the other hand, in the iron based system, exchange bias of $H_E \sim 3$ kOe have been reported [15] in partially oxidized iron thin films prepared by sputtering at very low temperatures which provides samples formed by nanoparticles with metallic iron and iron oxide mixed composition [16], where the core–shell (metal-oxide) microstructure has been univocally determined by conductive scanning force microscopy [17]. Furthermore, anisotropies up to $H_E \sim 6$ kOe have been obtained in iron nanoparticles prepared by the gas-phase aggregation technique, which have been described as a metallic iron core coated by γ-Fe_2O_3 [18].

In this work, we present a structural study based on X-ray absorption spectroscopy, to explain the magnetic properties (paying special attention to the variation of exchange bias) of iron-based nanoparticles prepared by the gas phase aggregation technique.

2. Experimental

Cluster-assembled films of iron have been prepared using a sputtering-based cluster source (from Mantis Deposition Ltd.) similar to the originally design by Haberland et al. [19], which is referred as the gas-phase aggregation technique. As shown in Fig. 1, this cluster source has two different parts, so-called aggregation and deposition chambers. The aggregation chamber contains a planar 2-in. magnetron sputtering source and consists in a water cooled steel bell with a small hole (~3 mm) through which the clusters leave. Since vacuum is made through this small hole and sputtering gases are introduced directly in the aggregation chamber, the magnetron works at relatively high pressure (10^{-1} mbar) in order to create the suitable environment for cluster aggregation. The deposition chamber, which has another hole aligned to the former one, is directly linked to another independent turbo pump system. The pressure in the deposition chamber during deposition is in the 10^{-3} mbar range, which allows clusters to travel from the aggregation chamber hole to the substrate, as well as to perform standard sputtering from another source. The variation of the cluster mean size depends on several parameters, such as cluster aggregation path length L_a (distance between the magnetron and the first hole), aggregation gases (Ar and He) flow rates, sputtering power, etc.

The iron cluster deposition mechanism can be described as follows. (i) Even if a He/Ar mixture is introduced in the aggregation chamber, only the Ar ions are capable to sputter atoms from the Fe target; (ii) the relatively high pressure in the aggregation chamber favours collisions between the sputtered Fe atoms and the Ar ones providing a divergent set of trajectories for Fe atoms; (iii) due to these trajectories, Fe atoms can join together forming Fe clusters before arriving to any surface; (iv) along this process, iron oxidation is extremely effective if a small oxygen content is present; (v) additionally, He flow increases the gas speed through the small aperture and favours the exit of clusters by reducing the remaining time at the aggregation chamber, which is a characteristic parameter to control average cluster size; (vi) on this way, clusters can reach a bigger size when the distance between the sputtering source and the chamber aperture becomes larger or, conversely, their size is smaller when a higher He flow makes Fe clusters travel from the sputtering source to the chamber aperture in a shorter time.

Before the sputtering process, the base pressure provided by the high vacuum system at the aggregation chamber of our system is in the range of 10^{-6} mbar. Even in the absence of intentionally introduced oxygen gas, these standard vacuum conditions and the allowed pressure inside the aggregation chamber during the sputtering process make possible some partial oxidation of the obtained clusters.

In order to prepare particles of different sizes, we have used several aggregation lengths. In this work, we report on samples prepared with two different lengths (L_a = 43 mm and L_a = 111 mm) which correspond to the limits of our experimental set up. Sputtering was driven by a DC-power source of about 2 W and the obtained clusters were deposited on Si(1 0 0) substrates at room temperature. An appropriate Ar/He mixed atmosphere of 5.0×10^{-1} mbar was achieved in the aggregation chamber by introducing Ar and He constant flows (50 sccm and 70 sccm, respectively).

With the aim of preventing further oxidation, as well as to isolate the deposited Fe-nanoparticles, a carbon layer was deposited on top of each cluster deposition, which allows fabrication of multilayered stacks by the consecutive repetition of clusters deposition followed by the carbon capping. In this case, carbon was deposited by using a DC-operated 2-inch planar magnetron located in the deposition chamber with an Ar pressure of 5.0×10^{-3} mbar and with a deposition rate of about 1 nm/min.

With these fabrication capabilities, we have studied the magnetic properties of iron clusters prepared with different aggregation lengths and under different oxidation conditions. First, the effect of the cluster size on the magnetic properties has been studied by preparing two samples with the shortest and largest aggregation lengths. For these samples some oxidation takes place in the aggregation chamber due to the very low oxygen residual pressure. Additionally, the effect of the oxidation after deposition has been investigated by exposing clusters to an oxygen atmosphere. For this purpose, two additional set of samples were prepared by the exposition to an O_2 flow at a pressure of 5×10^{-1} mbar for 30 min before capping with a carbon continuous layer. According to the different oxidation processes and aggregation lengths, multilayers labelled as $[^{AD}(n\text{-Fe})_{La}/C]_{10}$ account for ten periods formed by "as-deposited" clusters prepared with an L_a aggregation length and sputtered carbon and $[^{Ox}(n\text{-Fe})_{La}/C]_{10}$ account for ten periods of after deposition oxidized clusters and sputtered carbon.

The obtained size distribution was characterized by Atomic Force Microscopy (AFM). AFM measurements were made under ambient conditions using a commercial head and software [20] from Nanotec™. Commercial Nanosensors PPP-NCH-w tips with $k = 42$ N m^{-1} and $f_0 = 330$ kHz were used for topographic characterization using tapping mode.

Magnetic measurements were carried out in a SQUID magnetometer (MPMS-5, from Quantum Design). In order to study the possible exchange-bias effect, magnetization hysteresis loops were achieved up to 50 kOe at different temperatures, from 2 K to room temperature, after cooling the samples under an applied field of 20 kOe.

A thorough study of the short-range structure and the electronic configuration was performed by X-ray absorption spectroscopy (XAS) at the Fe K-edge. XAS spectra were measured in the fluorescence yield mode at the Spanish CRG beamline (SpLine, BM25) of the European Synchrotron Radiation Facility (ESRF). Energy was set using a Si(1 1 1) double crystal monochromator, detuned up to a 70% of maximum in order to reject contributions from higher harmonics.

Extended X-ray absorption fine structure (EXAFS) analysis was performed by using the VIPER program [21]. Oscillations were obtained after removing the background by a cubic spline fitting polynomial, EXAFS signal [$\chi(k)$] was obtained by normalizing the magnitude of the oscillations to the edge jump. The distribution function around iron atoms has been calculated by Fourier transforming the k^3-weighted EXAFS signal [$k^3\chi(k)$].

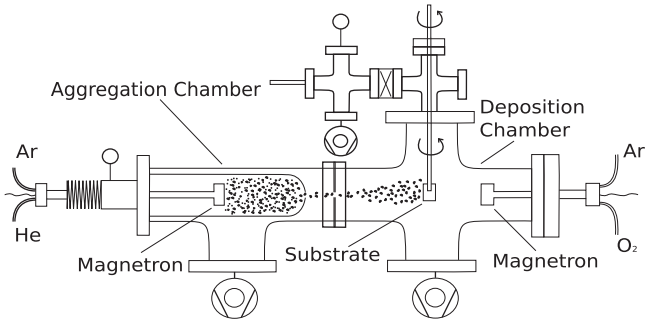

Fig. 1. Schematic drawing of the used cluster deposition system based on the gas aggregation technique.

3. Results and discussion

Freshly deposited clusters (without any additional capping layer) have been used for size characterization by AFM. Fig. 2 shows typical topographic images of samples prepared with two different aggregation path lengths (L_a = 43 mm and L_a = 111 mm). It should be noted that the L_a = 43 mm sample was prepared on Si(0 0 1) wafer and the L_a = 111 mm sample was deposited on gold capped (60 nm) Si(0 0 1), which explains the different aspect of the underside at the images. Even if a possible oxidation process could happen before taking sample away from the preparation chamber, AFM images depict clusters deposition of 3–4 nm size for L_a = 43 mm preparation and 6–8 nm for L_a = 111 mm, showing the expected enhancement of cluster size with increasing the aggregation length. Insets show the profile of two selected isolated clusters, where each characteristic size may be easily determine by its height on the flat substrate. It should be noted that AFM gives its best resolution only along the vertical direction, but lateral resolution is determined by the curvature radius of the tip (that typically is more than 10 nm), which may allow an apparent cluster shape different from the actual one.

Fig. 3 shows hysteresis loops (measured at 5 K after cooling down under an applied magnetic field of 20 kOe) corresponding to $[^{AD}(n\text{-Fe})_{111\,mm}/C]_{10}$, $[^{Ox}(n\text{-Fe})_{111\,mm}/C]_{10}$, $[^{AD}(n\text{-Fe})_{43\,mm}/C]_{10}$ and $[^{Ox}(n\text{-Fe})_{43\,mm}/C]_{10}$ multilayers. This set of samples let to study the influence of cluster oxidation in the obtained magnetic properties at two selected aggregation lengths (L_a = 111 mm and L_a = 43 mm). For comparison purposes, magnetization has been normalized to